Anomalously high thermoelectric figure of merit in $Bi_{1-x}Sb_x$ nanowires by carrier pocket alignment

Oded Rabin[a], Yu-Ming Lin,[b] and Mildred S. Dresselhaus[b),c),d)]
Massachusetts Institute of Technology, Cambridge, Massachusetts 02139-4307

(Received 12 February 2001; accepted for publication 24 April 2001)

Electronic transport calculations were carried out for $Bi_{1-x}Sb_x$ nanowires ($0 \leqslant x \leqslant 0.30$) of diameters $10\,\text{nm} \leqslant d_W \leqslant 100\,\text{nm}$ at 77 K. A band structure phase diagram was generated, showing the dependence of the relative band edge positions on diameter and composition. Calculations of the thermoelectric figure-of-merit (ZT) predict that the performance of $Bi_{1-x}Sb_x$ nanowires is superior to that of Bi nanowires and to that of the bulk alloy. An exceptionally high value of ZT for p-type nanowires at 77 K was found for $d_W \sim 40\,\text{nm}$ and $x \sim 0.13$, which is explained by the coalescence in energy of up to ten valence subband edges to maximize the density-of-states at the Fermi energy.

[DOI: 10.1063/1.1379365]

Thermoelectric (TE) devices are employed for the direct conversion of heat into electrical energy. Such a device is composed of a p-type leg and an n-type leg, in which the electric current and its conjugated thermal current flow in a parallel and an antiparallel fashion, respectively.[1,2] The efficiency of a TE device is determined by the Seebeck coefficient (S), the electric conductivity (σ), and the thermal conductivity (κ) of each of its components (''legs''). Commonly, materials are evaluated in terms of their dimensionless thermoelectric figure-of-merit, ZT, given by $ZT = \sigma S^2 T/\kappa$, where T is the absolute temperature. Previous theoretical studies of low dimensional systems for TE applications[3] have predicted an enhancement in ZT as the film thickness in two-dimensional (2D) systems[4] or the wire diameter in one-dimensional (1D) systems[5,6] is decreased. The ZT benefits both from quantum effects related to carrier confinement and from pronounced phonon scattering at the boundaries.

Fabrication of bismuth (Bi) nanowires has been demonstrated[7,8] and their transport properties are currently being studied.[8–10] Theoretical work on transport in Bi nanowires[6] has predicted that this system is a good candidate for an n-type leg for low temperature (77 K) performance. The ZT of a Bi nanowire, oriented along the trigonal crystallographic direction and properly doped, is expected to reach values of interest ($ZT \geqslant 1$ at 77 K) as the wire diameter (d_W) is decreased below 15 nm. Even smaller diameters, $d_W \approx 5$ nm, are needed for the Bi nanowires to serve as good p-type legs. However, the fabrication of uniform and high quality wires with $d_W \leqslant 15$ nm is very challenging.[8]

In this letter, we report calculations of the TE properties of the $Bi_{1-x}Sb_x$ alloy nanowire system, in which an unusual type of behavior is predicted. $Bi_{1-x}Sb_x$ alloys in bulk form show a versatile electronic behavior, ranging from semimetallic to direct and indirect band gap semiconducting,[11] depending on the antimony mole fraction, x. Also, the best ZT value of bulk $Bi_{1-x}Sb_x$ at low temperatures (e.g., 77 K) is higher than that of Bi, and higher than that of any other compound previously examined.[12] Here, the variation of x, together with the control over d_W, gives us additional control over the electronic band structure of the system, allowing higher ZT values to be obtained at larger wire diameters in $Bi_{1-x}Sb_x$ nanowires compared to Bi nanowires, particularly for p-type wires.

Numerical calculations were carried out to determine the 1D electronic subband structure of $Bi_{1-x}Sb_x$ nanowires with compositions $0 \leqslant x \leqslant 0.30$ at 77 K. The wires were treated as infinite cylinders with diameters $10\,\text{nm} \leqslant d_W \leqslant 100\,\text{nm}$, with their principal axis oriented along the trigonal crystallographic direction. Band parameters from bulk $Bi_{1-x}Sb_x$ at 77 K were used. The solutions for the energy eigenvalue problem in the transverse plane (2D confinement), with the electronic eigenfunctions forced to vanish at the wire boundary, were obtained numerically, as described previously.[6] The energy levels thus obtained are the minima of sets of 1D subbands. The nonparabolicity of the L-point carrier pocket dispersion relation was taken into account in calculating the carrier effective mass at the bottom of each subband, yet the wave vector dependence of the effective mass was neglected within each subband. The quantities σ, S, and the electronic contribution to the thermal conductivity (κ_{el}) were calculated from the electronic band structure using the semiclassical Boltzmann equation of motion within the constant relaxation time approximation.[13] The experimental values for the mobilities of the L- and T-point pocket carriers in bulk Bi and of the H-point pocket carriers in bulk Sb were used. The mobilities in the alloys have been determined experimentally only for a number of Bi-rich compositions, are sensitive to the sample quality,[14–16] and are hard to predict. The lattice contribution to the thermal conductivity was obtained, in accordance with Matthiesen's law, by fitting experimental results[17,18] to the formula $\kappa_{\text{ph}}^{-1} = \kappa_0^{-1} + \kappa_1^{-1} x$, where κ_0 and κ_1 are constants. This fit is appropriate up to $x \sim 0.25$, where κ_{ph} begins to increase with Sb concentration. At a given d_W and x, the transport properties σ, S and $\kappa = \kappa_{\text{el}} + \kappa_{\text{ph}}$ were

[a)]Department of Chemistry.
[b)]Department of Electrical Engineering and Computer Science.
[c)]Department of Physics.
[d)]Electronic mail: millie@mgm.mit.edu

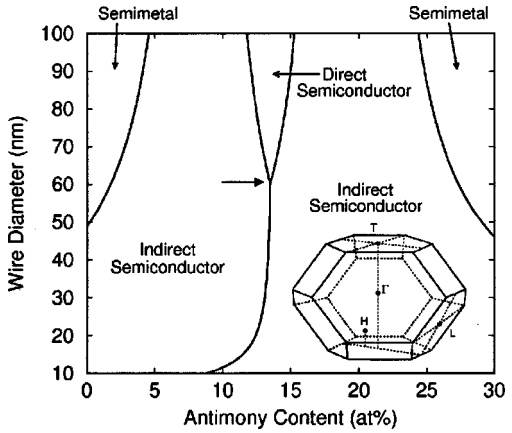

FIG. 1. Phase horizontal diagram of the electronic band structure of $Bi_{1-x}Sb_x$ nano- wires. The bold horizontal arrow in the center points at the condition where the ten hole pockets [about the T-point, the three L-points, and the six H-points in the Brillouin zone (see inset)] coalesce in energy.

evaluated as a function of the position of the Fermi level, and ZT was obtained from these quantities.

The ZT dependence on the position of the Fermi level in the nanowires shows one maximum at carrier concentrations that correspond to an excess of negative carriers (denoted by $Z_{n,\mathrm{opt}}T$) and one or two maxima at carrier concentrations corresponding to an excess of holes (the highest among them denoted by $Z_{p,\mathrm{opt}}T$). The maxima normally occur when the Fermi level is in the vicinity of the band edge of the first subband originating from one of the carrier pockets at the L, T, or H points of the Brillouin zone (see inset in Fig. 1).

Figure 1 depicts the rich variety of electronic band structures predicted for the $Bi_{1-x}Sb_x$ nanowire system as a function of d_W and x. The semimetal and the indirect gap semiconductor alloys in the low antimony content region ($x \lesssim 0.13$) have their highest valence band extremum at the T point, while those alloys with higher x ($x \gtrsim 0.13$) have their H-point hole pockets at the highest energy. Along the solid lines in this ''phase diagram,'' the extrema of the first subband of carrier pockets at two different points in the Brillouin zone coalesce in energy. The bold horizontal arrow in the center of the diagram points to the particularly interesting situation where the extrema of all 10 hole pockets coalesce in energy ($d_W = 60\,\mathrm{nm}$, $x = 0.13$), resulting in a high density of states which is beneficial for increasing the magnitude of the Seebeck coefficient (*vide infra*). This diagram also predicts a shift to higher values of the critical diameter at which the overlap between the L-point electron subbands and the T-point hole subbands vanishes (semimetal-to-semiconductor transition)[8,19] as Sb is added to pure Bi nanowires. The transition to a narrow-gap semiconductor benefits the TE behavior, since in the semimetallic phase, carriers of opposite signs make canceling contributions to S. We therefore expect to obtain higher ZT values at larger diameters in $Bi_{1-x}Sb_x$ nanowires when compared to Bi nanowires. Last, the direct band gap phase, which exists in the bulk for 9%–17% Sb, is reduced to a narrower range in the nanowires and ceases to exist for $d_W \leqslant 60\,\mathrm{nm}$. This limits the increase in ZT that can be gained from the high density of states obtained from the reduction to a 1D system due to the lower contribution of the high-mobility holes at the L-point pockets for p-type TE legs.

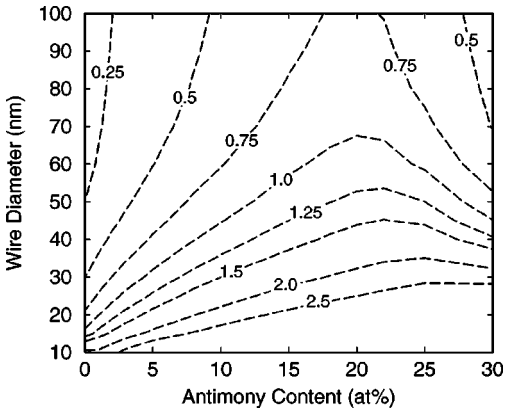

FIG. 2. Contour plot of the optimal ZT values for n-type $Bi_{1-x}Sb_x$ nanowires vs wire diameter and antimony concentration. The contour lines were generated using MATLAB from a grid of 323 point calculations.

The contour plot of $Z_{n,\mathrm{opt}}T$ for $Bi_{1-x}Sb_x$ in Fig. 2 reflects the trends previously observed in Bi nanowires.[6] The value of $Z_{n,\mathrm{opt}}T$ increases as the wire diameter decreases, for all values of x. As the content of Sb at constant d_W is increased, $Z_{n,\mathrm{opt}}T$ increases until a certain optimal value of x (dependent on d_W) at which a maximum is reached. The dependence on d_W is explained by two main factors: (i) As the system is reduced from a three-dimensional (bulk) to a 1D system (nanowire), the electronic structure evolves into one consisting of a set of subbands. The diverging density of states at the extrema of a 1D band leads to high values of S and of ZT. (ii) The spatial confinement of carriers in the nanowire shifts the band edge energies, inducing a semimetal-to-semiconductor transition. The undesirable contribution of the minority carriers that lowers the magnitude of S is further reduced by the proper positioning of the Fermi level. The dependence on x is a consequence of two additional factors: (i) Bulk $Bi_{1-x}Sb_x$ is semiconducting for $0.07 \leqslant x \leqslant 0.22$, with a maximum band gap at $x = 0.17$, and displays its best TE performance in this range.[18,20] (ii) The large mass difference between the atomic components of the Bi–Sb alloy gives rise to efficient scattering of phonons, thereby lowering κ_{ph} with increasing x, while the carrier mobilities only slightly decrease as long as $x < 0.10$.

While mostly complying with these trends, the contour plot of $Z_{p,\mathrm{opt}}T$ for p-type $Bi_{1-x}Sb_x$ nanowires in Fig. 3

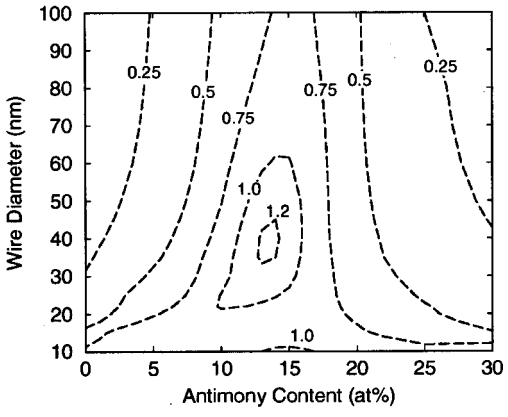

FIG. 3. Contour plot of the optimal ZT values for p-type $Bi_{1-x}Sb_x$ nanowires vs wire diameter and antimony concentration. The contour lines were generated using MATLAB from a grid of 323 point calculations.

shows a significant deviation relative to $Z_{n,\mathrm{opt}}T$: a local maximum is found for $0.13 \leqslant x \leqslant 0.14$ and $35\,\mathrm{nm} \leqslant d_W \leqslant 45\,\mathrm{nm}$, with a predicted $Z_{p,\mathrm{opt}}T$ value higher than 1.2 at 77 K. As seen in the plot, such high values of ZT in p-type materials are not expected for any other p-type $Bi_{1-x}Sb_x$ alloy at wire diameters above 10 nm. Unexpectedly, $Z_{p,\mathrm{opt}}T$ does not increase monotonically as d_W decreases.

To understand the source of this unprecedented enhancement in $Z_{p,\mathrm{opt}}T$, we examined the electronic band structure in the $Bi_{1-x}Sb_x$ nanowire system (see Fig. 1). Of interest are the valence subband extrema, which occur at the three L-points, one T-point, and six H-points of the Brillouin zone. The enhancement in $Z_{p,\mathrm{opt}}T$ is observed near the merging of the edges of the ten hole pockets, and along the boundary between the two indirect gap semiconductor phases. These degeneracies lead to an increased density of states near the Fermi energy for valence band carriers in p-type $Bi_{1-x}Sb_x$ nanowires, which in turn is manifested by exceptionally high values of $Z_{p,\mathrm{opt}}T$. Another factor contributing to the appearance of the maximum in $Z_{p,\mathrm{opt}}T$ is the relative weight of the high mobility L-point holes in the total carrier concentration. The ZT of n-type $Bi_{1-x}Sb_x$, for which only L-point electron carriers exist, is higher than that of p-type $Bi_{1-x}Sb_x$ where various carrier pockets contribute to transport. Thus, the contribution of the L-pocket carriers to the enhancement of ZT is the most important. In the studied region, at the conditions for optimal Z_pT, our calculations suggest that the L-point hole population reaches a maximum of 28% of the total hole population for $x=0.12$ and $d_W=100\,\mathrm{nm}$. It drops to 7% of the total hole population as x increases to 0.165 or as d_W decreases to 15 nm. The depletion of the L-point hole population with increasing x for $x \geqslant 0.12$ is in agreement with the observation that, for a given wire diameter, the peak in $Z_{p,\mathrm{opt}}T$ occurs at lower concentrations of Sb than the peak in $Z_{n,\mathrm{opt}}T$. It may also explain the existence of the local maximum as an interplay between the lower population of the L-point hole pockets and a higher subband edge density-of-states, as we decrease the diameter of the $Bi_{1-x}Sb_x$ nanowires.

The main weakness of our model is the lack of information regarding the mobilities of the different carriers as a function of alloy composition. However, it provides us with valuable insight into the effect of Sb alloying in the Bi nanowire system. Mobility studies will also need to be extended to nanowire systems, since along the ''phase transition'' lines, intervalley scattering processes might play a dominant role, strongly influencing the mobilities and ZT.[21] Thus, the values observed here represent an optimistic estimate for the TE performance of this nanowire system.

In summary, the theoretical study of the $Bi_{1-x}Sb_x$ nanowire system predicts high values of ZT for both p-type and n-type materials at 77 K. An unprecedented enhancement in $Z_{p,\mathrm{opt}}T$ is expected even at wire diameters of 40 nm, a diameter that can be readily achieved by current methods of fabrication of nanowire arrays. The enhancement is attributed to the coalescence in energy of the subband edges of the ten hole pockets of this system and the resulting high density of states. This phenomena may not be limited to $Bi_{1-x}Sb_x$, and could serve as a strategy for the enhancement of ZT in other low-dimensional systems. Of practical interest is the fact that the same basic nanowires, under different doping conditions, can be used as either p-type or n-type legs in a TE device with $ZT>1.2$ at low temperature.

The authors thank Dr. G. Dresselhaus and S. B. Cronin for valuable discussions. Support from MURI Subcontract No. 0205-G-7A114-01, NSF Grant No. DMR-98-047334, and U.S. Navy Contract No. N00167-92-K005 is gratefully acknowledged.

[1] H. J. Goldsmid, *Thermoelectric Refrigeration* (Plenum, New York, 1964).
[2] A. F. Ioffe, *Semiconductor Thermoelements and Thermoelectric Cooling* (Infosearch, London, 1956).
[3] M. S. Dresselhaus, Y.-M. Lin, S. B. Cronin, O. Rabin, M. R. Black, G. Dresselhaus, and T. Koga, in *Semiconductors and Semimetals: Recent Trends in Thermoelectric Materials Research III*, edited by T. M. Tritt (Academic, San Diego, 2001), Chap. 1, pp. 1–121.
[4] T. Koga, X. Sun, S. B. Cronin, and M. S. Dresselhaus, Appl. Phys. Lett. **73**, 2950 (1998); *ibid.*. **75**, 2438 (1999); T. Koga, T. C. Harman, S. B. Cronin, and M. S. Dresselhaus, Phys. Rev. B **60**, 14286 (1999); T. Koga, O. Rabin, and M. S. Dresselhaus, Phys. Rev. B **62**, 16703 (2000).
[5] X. Sun, Z. Zhang, and M. S. Dresselhaus, Appl. Phys. Lett. **74**, 4005 (1999).
[6] Y.-M. Lin, X. Sun, and M. S. Dresselhaus, Phys. Rev. B **62**, 4610 (2000).
[7] Z. Zhang, D. Gekhtman, M. S. Dresselhaus, and J. Y. Ying, Chem. Mater. **11**, 1659 (1999); T. E. Huber, M. J. Graf, C. A. Foss, Jr., and P. Constant, J. Mater. Res. **15**, 1816 (2000); K. Liu, C. L. Chien, P. C. Searson, and K. Yu-Zhang, Appl. Phys. Lett. **73**, 1436 (1998).
[8] J. Heremans, C. M. Thrush, Y.-M. Lin, S. Cronin, Z. Zhang, M. S. Dresselhaus, and J. F. Mansfield, Phys. Rev. B **61**, 2921 (2000).
[9] J. Heremans, C. M. Thrush, Z. Zhang, X. Sun, M. S. Dresselhaus, J. Y. Ying, and D. T. Morelli, Phys. Rev. B **58**, R10091 (1998).
[10] Y.-M. Lin, S. B. Cronin, J. Y. Ying, M. S. Dresselhaus, and J. P. Heremans, Appl. Phys. Lett. **76**, 3944 (2000).
[11] A. L. Jain, Phys. Rev. **114**, 1518 (1959).
[12] D. M. Rowe, *CRC Handbook of Thermoelectrics* (CRC Press, New York, 1995).
[13] N. W. Ashcroft and N. D. Mermin, *Solid State Physics* (Saunders College, Philadelphia, 1976).
[14] H. J. Goldsmid, Phys. Status Solidi A **1**, 7 (1970).
[15] T. Yazaki and Y. Abe, J. Phys. Soc. Jpn. **24**, 290 (1968).
[16] A. Demouge, B. Lenoir, Yu. Ravich, H. Scherrer, and S. Scherrer, J. Phys. Chem. Solids **56**, 1155 (1995).
[17] V. D. Kagan and N. A. Red'ko, Proceedings of the 14th IEEE International Conference on Thermoelectrics, St. Petersburg, Russia, 1995, p. 78.
[18] W. M. Yim and A. Amith, Solid-State Electron. **15**, 1141 (1972).
[19] C. A. Hoffman, J. R. Meyer, F. J. Bartoli, A. Di Venere, X. J. Yi, C. L. Hou, H. C. Wang, J. B. Ketterson, and G. K. Wong, Phys. Rev. B **48**, 11431 (1993).
[20] B. Lenoir, A. Dauscher, X. Devaux, R. Martin-Lopez, Yu. I. Ravich, H. Scherrer, and S. Scherrer, Proceedings of the 15th IEEE International Conference on Thermoelectrics, Pasadena, CA, 1996, p. 1.
[21] B. Lenoir, A. Dauscher, M. Cassart, Yu. I. Ravich, and H. Scherrer, J. Phys. Chem. Solids **59**, 129 (1998).